A new approach for the spatially resolved qualitative analysis of the protein distribution in hydrogel beads based on confocal laser scanning microscopy

Heinemann, Matthias; Wagner, Thomas; Doumèche, Bastien; Ansorge-Schumacher, Marion; Büchs, Jochen

Published in:
Biotechnology Letters

DOI:
10.1023/A:1015558823726

Publication date:
2002

Biotechnology Letters **24:** 845–850, 2002.

A new approach for the spatially resolved qualitative analysis of the protein distribution in hydrogel beads based on confocal laser scanning microscopy

Matthias Heinemann[1], Thomas Wagner[1], Bastien Doumèche[2], Marion Ansorge-Schumacher[2] & Jochen Büchs[1,*]

Departments of [1]Biochemical Engineering and [2]Biotechnology, Aachen University of Technology, 52056 Aachen, Germany

[*]Author for correspondence (Fax: +49 241 8022265; E-mail: buechs@biovt.rwth-aachen.de)

Received 6 february 2002; Revisions requested 20 February 2002; Revisions received 11 March 2002; Accepted 12 March 2002

Key words: alginate, confocal laser scanning microscope, immobilization, protein distribution, white egg albumin

Abstract

To investigate the spatial distribution of white egg albumin (WEA) in alginate beads, a new method based on confocal laser scanning microscopy (CLSM) was developed. In contrast to the existing CLSM methods, misleading conclusions are prevented with the application of the new method which does not allow the attenuation of the exciting and emitted light by the opaque hydrogel matrices to be disregarded. By the application of this method, the distribution of WEA in alginate beads was shown to be dependent on the amount of protein loading. At low quantities of protein, a higher protein concentration occurs in the shell layer of the alginate bead while at higher loadings a more or less homogeneous distribution is observed.

Introduction

Alginate beads are promising tools to immobilize enzymes for biocatalysis in organic solvents (Hertzberg *et al.* 1992, Koch & Hartmeier 1995). Rational design of processes with immobilized enzymes can be accomplished by using mathematical models describing mass transfer and enzymatic reaction kinetics inside the immobilization matrix. A precise modeling of the enzymatic reaction kinetics requires the knowledge of the local enzyme concentration in the immobilization bead (Guisan *et al.* 1987) as the local maximum velocity of the reaction, $v_{max}(r)$, depends on the local enzyme concentration, $c_E(r)$, and the specific turnover number of the enzyme, k_{cat}.

Investigations of the cross-sectional distributions of proteins in various immobilization matrices have been carried out for several years (Carleysmith *et al.* 1980, Guisan *et al.* 1987, Lasch *et al.* 1972). Most often, the matrices with the embedded fluorescent-labeled protein were cut into thin slices which were subsequently analyzed with a fluorescent microscope. Higher spatial resolutions, however, can be achieved by the application of modern non-invasive measurement techniques such as confocal laser scanning microscopy. This kind of microscope is distinguished by special optics to non-destructively produce optical slices with a high resolution of a three-dimensional specimen. Thus, spatial information about the distribution of fluorescent compounds (e.g. fluorescently labeled protein) over the radius of an immobilization bead can be obtained.

Up to now, only a few papers have been published, in which a confocal laser scanning microscope has been used for the analysis of fluorescent compounds in macroscopic large objects, such as matrices for biocatalyst immobilization or chromatographic protein separation (Pinto & Macías 1995, Ljunglöf & Thömmes 1998, Laca *et al.* 1999). In these papers, the spatial protein distribution inside the matrices was gained by the analysis of the fluorescence intensity distribution of a single horizontal optical slice obtained from the

middle of the spherical object. However, the application of this procedure with spherical opaque objects can lead to wrong conclusions because of the radially uneven attenuation of the exciting and emitted light (Rademann *et al.* 2001).

In this paper, a new method for the qualitative determination of the protein distribution in hydrogel beads will be presented. It is also based on a confocal laser scanning microscope but circumvents the mentioned drawback of the existing method.

Materials and methods

Protein labeling

Purified white egg albumin WEA (Fluka) was stained by covalent attachment of a fluorescent dye. The FluoReporter Oregon Green 514 Protein Labeling Kit from Molecular Probes (Leiden, Netherlands) was used according to the instructions provided by the manufacturer. Oregon Green, a fluorescein derivative, has its excitation maximum at 514 nm with its emission maximum at 534 nm.

Bead production

Thirty-five ml of a 2% (w/v) alginate solution in 0.1 M Tris/HCl buffer, pH 7.5, was added dropwise into 400 ml of a 2% (w/v) $CaCl_2$ solution with the same buffer. A special bead forming device (Encapsulator, Inotech, Switzerland) was used to obtain beads with a diameter between 200 to 300 μm. Ten ml of the alginate solution contained 1.9 mg labeled protein whereas the remaining 25 ml alginate solution did not hold any protein. Therefore, in the hardening bath beads were initially present with and without labeled protein. By diffusive transport, however, the beads with protein released a quantity of protein into the hardening bath while the empty beads took up a certain amount of the released protein. Due to the slow rate of bead formation, the beads had different residence times in the hardening bath. This procedure was applied in order to produce alginate beads with a wide range of different protein loadings. After approx. 60 min in the hardening bath, the beads were removed with a filter, shortly dried with a paper towel and transferred into hexane. Because of the insolubility of the protein in hexane (Hertzberg *et al.* 1992), a further leakage of protein from the beads to the hexane phase is prevented. The applied procedure for the bead production resulted in a maximum range of different protein loadings from 0 to 0.19 mg ml^{-1}. The beads were kept in the hexane phase for at least two weeks before the actual confocal analysis to allow the protein distribution inside the beads to reach equilibrium.

Instrumentation and confocal analysis

The experimental analysis was performed with a Leica confocal microscope TCS SP (Heidelberg, Germany) equipped with an argon/krypton laser with possible excitation at 476, 488, 568 and 647 nm. The fluorescent dye was excited at 488 nm (42% of maximum absorption at 514 nm) and the emitted light was recorded with a photomultiplier between 510–550 nm. For the confocal analysis, a small number of alginate beads which contained the fluorescent labeled protein were placed in a self-build chamber which was filled with hexane. A 20× water immersion objective (Leica HCX APO, L20×/0.50 W U-V-I, Heidelberg, Germany) with a working distance of 3.5 mm was used which allowed a field of view of 0.5×0.5 mm. The images were recorded at a resolution of 512×512 pixels and analyzed by the supplied Leica confocal software (version 2.0, Heidelberg, Germany).

Method for the spatially resolved analysis of the protein distribution in hydrogel beads

With a confocal laser scanning microscope, optical slices can be gathered non-invasively from macroscopic large objects. The obtained spatial distribution of fluorescence in optical slices of opaque spherical objects, however, most often does not represent the real existing spatial distribution of fluorescence. This can lead to wrong conclusions (Rademann *et al.* 2001). The potential discrepancy between the apparent and the real distribution is caused by the radially different attenuation of the emitted light due to the radially different path lengths of the light through the top hemisphere of the bead (i.e. the object matter above the current optical slice). The new method circumvents the risk of wrong conclusions when analyzing the spatial distribution of fluorescent compounds in macroscopic large spherical objects with a confocal laser scanning microscope.

Principle

For the new method, a series of horizontal optical slices through a single bead, loaded with fluorescent labeled protein, is acquired which results in a stack of

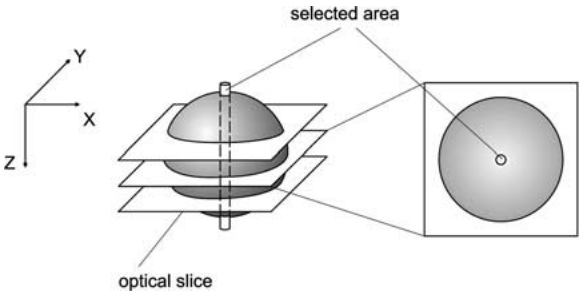

Fig. 1. Schematic drawing demonstrating the principle of the new method.

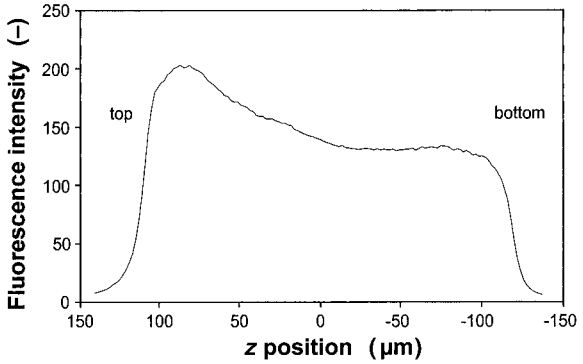

Fig. 2. Translation of the mean fluorescence intensities of the selected area obtained from the optical slices into a fluorescence intensity profile over the bead radius (in z direction).

images (see Figure 1). Subsequently, a small circular area in the middle of the bead cross-section (130 pixels) is selected and the mean fluorescence intensity of this area in every single image of the stack is determined. By plotting the determined mean fluorescence intensities over the z position of the according optical slice, an intensity profile over the bead diameter (in z direction) will be obtained. As an example, a fluorescence intensity profile is presented in Figure 2.

It can be seen that the fluorescence intensity is diminishing with increasing depth of the optical slice. The decrease of fluorescence intensity is caused by the attenuation of the exciting and emitted light by the opaque alginate matrix (Visser *et al.* 1991). However, despite the fact that the intensity of the emitted light is decreasing with increasing depth, it is obvious from Figure 2, that at the bottom of the outer bead shell (around the z position -100) the fluorescence intensity increases again. This is a clear evidence for an inhomogeneous spatial distribution of the fluorescent labeled protein in the alginate matrix, where a higher concentration of the protein is present in the outer bead shell.

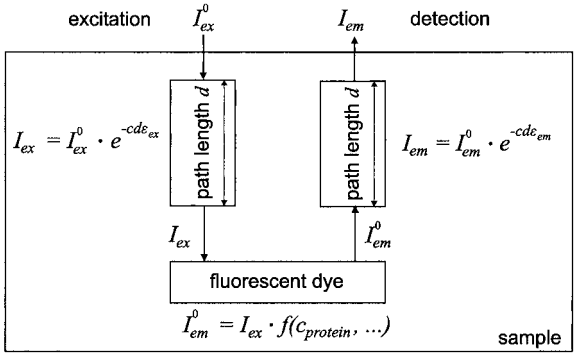

Fig. 3. Presentation of the equations for the correction algorithm.

Correction of the attenuation

To obtain a non-attenuated intensity profile, a correction algorithm was developed. The degree of the light attenuation can be described by the Lambert–Beer law

$$I = I^0 \cdot e^{-cd\varepsilon}, \tag{1}$$

where I represents the attenuated light intensity, I^0 the original, non-attenuated light intensity, ε the wavelength dependent absorptivity coefficient, c the concentration of the absorbing species (here: alginate) and d the path length of the light through the sample. The original intensity of the exciting laser light I_{ex}^0 and the original intensity of the emitted light I_{em}^0 are attenuated with the respective absorptivity coefficients $\varepsilon_{\mathrm{ex}}$ and $\varepsilon_{\mathrm{em}}$ on their way through the sample as it is illustrated in Figure 3. At the scanning depth d, the attenuated intensity of the exciting light I_{ex} determines the intensity of the emitted light I_{em}^0 together with other factors such as the concentration of the fluorescent labeled protein and parameters of the microscope and the dye.

By combining the equations presented in Figure 3, the following correlation for the attenuated, emitted intensity I_{em} acquired from the scanning depth d_1 can be obtained:

$$I_{\mathrm{em}}(d_1) = I_{\mathrm{ex}}^0 \cdot f(c_{\mathrm{protein}}(d_1), \ldots) \cdot e^{-cd_1(\varepsilon_{\mathrm{em}}+\varepsilon_{\mathrm{ex}})}. \tag{2}$$

Analogous, the attenuated, emitted intensity from depth d_2 is given by

$$I_{\mathrm{em}}(d_2) = I_{\mathrm{ex}}^0 \cdot f(c_{\mathrm{protein}}(d_2), \ldots) \cdot e^{-cd_2(\varepsilon_{\mathrm{em}}+\varepsilon_{\mathrm{ex}})}. \tag{3}$$

For the correction algorithm, it is assumed that the depths d_1 and d_2 are the two scanning depths representing the same bead radius at the top (d_1) and the bottom (d_2) of the bead. With the additional assumption of a radially symmetrical distribution of the

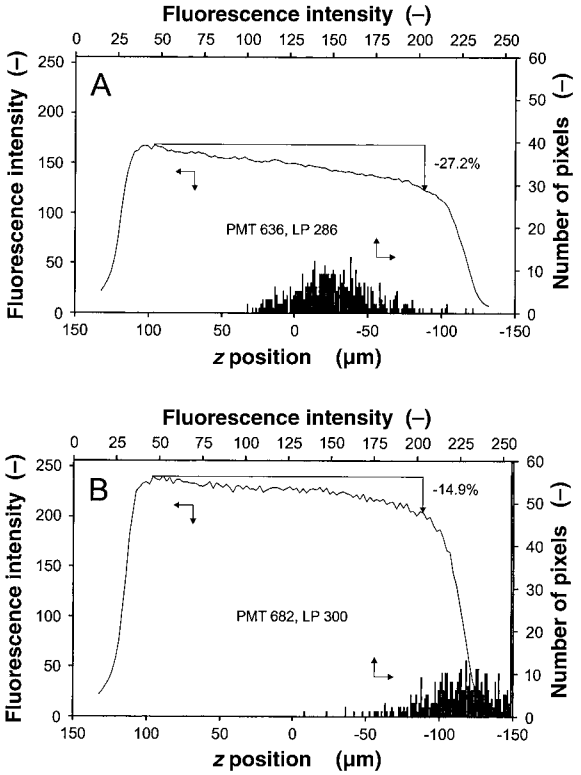

Fig. 4. Demonstration of the importance of correct settings of the laser power (LP) and the sensitivity of the photomultiplier (PMT); settings: (A) PMT 636, LP 286; (B) PMT 682, LP 300; primary axes: obtained intensity profiles with the respective settings; secondary axes: fluorescence intensity histograms obtained from the respective profile at position $z = 0$.

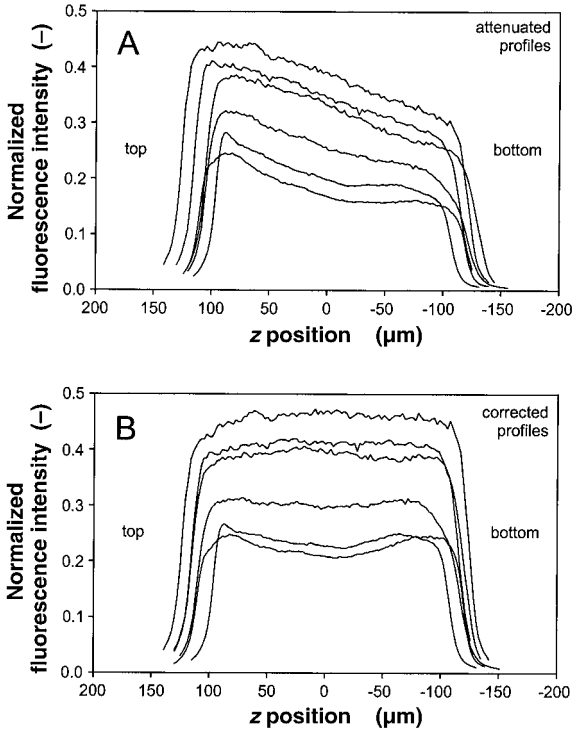

Fig. 5. (A) Attenuated intensity profiles obtained from beads with various protein loadings; (B) intensity profiles corrected for the attenuation.

fluorescent labeled protein over the bead radius, this leads to

$$c_{\text{protein}}(d_1) = c_{\text{protein}}(d_2). \tag{4}$$

Finally combining Equations (2), (3) and (4), the following correlation for the attenuation factor $-c(\varepsilon_{\text{ex}} + \varepsilon_{\text{em}})$ can be obtained:

$$-c(\varepsilon_{\text{ex}} + \varepsilon_{\text{em}}) = \frac{\ln\left(\dfrac{I_{\text{em}}(d_2)}{I_{\text{em}}(d_1)}\right)}{d_2 - d_1}\,. \tag{5}$$

With Equation (5) and the experimental data, the actual attenuation factor can be determined. By using this factor and Equation (2), the whole measured intensity profile can be corrected for the attenuation.

The proposed correction algorithm is only a first approximation because it assumes a constant alginate concentration c over the bead radius. However, it was shown that the distribution of alginate within the gelated bead is generally not uniform. Due to the gelling process, the beads show a high concentration at the surface which gradually decreases towards the center (Skjåk-Bræk *et al.* 1986).

Importance of correct settings of confocal laser scanning microscope

For the correct application of the presented method, a suitable laser power (LP) for the excitation and an appropriate sensitivity of the detector (photomultiplier, PMT) have to be chosen. If the laser power and the PMT sensitivity are set at too high values, misleading results can be obtained in such a manner that an inhomogeneous protein distribution will be recognized as a homogeneous distribution.

When a high laser power and a high PMT sensitivity are chosen, the recorded intensity signal might reach its system-dependent maximum level of 255. The value of 255 will be attributed to all intensities which might be even higher. Subsequently, this recorded intensity signal does not contain any relative information anymore compared to other signals. This dependence is illustrated in Figure 4 where a fluorescence intensity profile is recorded at two settings A

and B of the laser power and photomultiplier. Higher values have been selected for the recording of graph B. The comparison of the two graphs shows that the intensity profile changes in such a manner that the relative intensity reduction between two points of the same radius decreases with increased values for laser power and PMT sensitivity. In the limiting case of an extremely high laser power and PMT sensitivity, the obtained fluorescence profile will be horizontal.

This effect can be further illustrated by the fluorescence intensity histograms presented on the secondary axes in Figure 4. The histogram indicates the number of pixels with a specific intensity in the selected area of the optical slice obtained from the position $z = 0$. From the histogram in Figure 4B it can be seen, that with a high laser power and a high detector sensitivity the Gaussian distribution of the intensities are shifted to the right side. All the pixels with a theoretically higher value than 255 accumulate at this value which is indicated by the thick bar at the right side of Figure 4B. Therefore, to avoid misleading results the laser power and the PMT sensitivity have to be set in a way that the fluorescent intensity histogram lays in the middle of the whole range of the fluorescence intensity.

Further problems are caused by frequent system-dependent variations of the laser power (Zucker & Price 2001). A normalization of the obtained fluorescence intensities was therefore achieved by dividing the fluorescence intensity by the current laser power.

Presentation of exemplary results

In Figure 5, various fluorescence intensity profiles are presented as an example. Figure 5A shows the originally obtained attenuated profiles, whereas Figure 5B displays the respective corrected profiles. The profiles were obtained from a series of alginate beads containing different amounts of fluorescent labeled protein. Some of the corrected profiles show an even intensity distribution. Generally, these profiles have a higher normalized intensity level (>0.3) and therefore a higher protein loading. Profiles from beads with a lower normalized intensity level (<0.3) present an inhomogeneous intensity distribution with two maximums at the outer shell of the bead. This observation demonstrates that the spatial distribution of the protein WEA is obviously dependent on the amount of protein loading: Beads with a higher intensity level show a more or less even distribution, whereas in beads with a lower intensity level the protein is distributed inhomogeneously.

With the results of Longo *et al.* (1992) and Martinsen *et al.* (1992), who reported that protein can freely diffuse in an alginate matrix, it was expected that the protein WEA distributes evenly over the bead radius. Taking into account the findings of Skjåk-Bræk *et al.* (1986) of a higher concentration of alginate at the outer shell of the bead than in the middle, the observed inhomogeneous protein distribution at lower protein loadings leads to the assumption of a certain affinity of the protein WEA to the alginate matrix. Accordingly, an even distribution of protein over the whole bead cross-section will be obtained at high protein concentrations, when all the positions for the protein-alginate interaction are saturated. This hypothesis is supported by the results of Imeson *et al.* (1977) who found weak electrostatic interactions between the protein bovine serum albumin and the carboxyl groups of the polysaccharide chains of the alginate matrix. Therefore, conceivable artifacts such as a potential interaction of the fluorescent label with the alginate matrix can almost be excluded.

Transferred to enzymatically active proteins, the inhomogeneous protein distribution, with a higher concentration located at the outer bead shell, results in higher efficiencies compared to the same amount of a homogeneously distributed enzyme. This is caused by the shorter length of the diffusion path of the substrates (Borchert & Buchholz 1984, Guisan *et al.* 1987).

Conclusion

A new method was developed for the qualitative determination of the distribution of fluorescently labeled protein in hydrogel matrices. The most prominent advantage of the new method is the fact that it does not allow to disregard the attenuation of the exciting and emitted light by the opaque hydrogel matrix. Consequently, misleading conclusions are prevented.

However, the method still requires further optimization. The inhomogeneity of the alginate distribution has to be included in the algorithm which corrects the obtained fluorescence profile from the attenuation of light by the opaque alginate matrix. Moreover, for a quantitative analysis of the protein distribution with a confocal laser scanning microscope, substantial work is still necessary. The revealed instability of the power of the exciting laser is a known problem with confo-

cal laser scanning microscopes and makes a reliable quantitative analysis difficult.

Although the main concern of this work has been to study the methodology, an unexpected result concerning the protein distribution was obtained by the first application of the new method. It has been demonstrated that the distribution of WEA in alginate beads is dependent on the amount of protein loading. This lead to the assumption of a specific affinity of the white egg albumin for the alginate matrix.

Acknowledgement

The authors gratefully acknowledge the financial support of the Deutsche Forschungsgemeinschaft (DFG) within the Collaborative Research Center (SFB) 540 'Model-based experimental analysis of kinetic phenomena in fluid multiphase reaction systems'.

References

Borchert A, Buchholz K (1984) Improved biocatalyst effectiveness by controlled immobilization of enzymes. *Biotechnol. Bioeng*. **26**: 727–736.

Carleysmith SW, Eames MBL, Lilly MD (1980) Staining method for determination of the penetration of immobilized enzyme into a porous support. *Biotechnol. Bioeng.* **22**: 957–967.

Guisan JM, Serrano J, Melo FV, Ballesteros A (1987) Mixed enzymic reaction – internal diffusion kinetics of nonuniformly distributed immobilized enzymes. *Appl. Biochem. Biotech.* **14**: 49–72.

Hertzberg S, Kvittingen L, Anthonsen T, Skjåk-Bræk G (1992) Alginate as immobilization matrix and stabilizing agent in a two-phase liquid system: application in lipase-catalysed reactions. *Enzyme Microb. Tech.* 14: 42–47.

Imeson AP, Ledward DA, Mitchell JR (1977) On the nature of the interaction between some anionic polysaccharides and proteins. *J. Sci. Food Agr.* **28**: 661–668.

Koch M, Hartmeier W (1995) Enzymatic catalysis in organic media: reactors with solidified water-phase. In: Schmid R, ed. *Biochemical Engineering* 3, Stuttgart: Verlag Kurz, pp. 58–60.

Laca A, García LA, Argüeso F, Díaz M (1999) Protein diffusion in alginate beads monitored by confocal microscopy. The application of wavelets for data reconstruction and analysis. *J. Ind. Microbiol. Biot.* **23**: 155–165.

Lasch J, Iwig M, Hanson H (1972) Method of visualization of matrix-bound proteins. *Eur. J. Biochem.* **27**: 431–435.

Ljunglöf A, Thömmes J (1998) Visualising intraparticle protein transport in porous adsorbents by confocal microscopy. *J. Chromatogr.* **A813**: 387–395.

Longo MA, Novella IS, García LA, Díaz M (1992) Diffusion of proteases in calcium alginate beads. *Enzyme Microb. Tech.* **14**: 586–590.

Martinsen A, Storrø I, Skjåk-Bræk G (1992) Alginate as immobilization material: III. Diffusional properties. *Biotechnol. Bioeng.* **39**: 186–194.

Pinto MC, Macías P (1995) Determination of intraparticle immobilized enzyme distribution in porous support by confocal scanning microscopy. *Biotechnol. Tech.* **9**: 481–486.

Rademann J, Barth M, Brock R, Egelhaaf HJ, Jung G (2001) Spatially resolved single bead analysis: homogeneity, diffusion, and adsorption in cross-linked polystyrene. *Chem. Eur. J.* **7**: 3884–3889.

Skjåk-Bræk G, Smidsrød O, Larsen B (1986) Tailoring of alginates by enzymatic modification in vitro. *Int. J. Biol. Macromol.* **8**: 330–336.

Visser TD, Groen FCA, Brakenhoff GJ (1991) Absorption and scattering correction in fluorescence confocal microscopy. *J. Microsc.* **163**: 189–200.

Zucker RM, Price O (2001) Evaluation of confocal microscopy system performance. *Cytometry* **44**: 273–294.